Technical University of Denmark

DTU

Analytical gradients of wind turbine towers fatigue loads

Tibaldi, Carlo; Hansen, Morten Hartvig; Stolpe, Mathias

DTU Library
Technical Information Center of Denmark

DTU Wind Energy

DTU

Analytical gradients of wind turbine towers fatigue loads

Department of
Wind Energy
Report 2016

Carlo Tibaldi, Morten H. Hansen and Mathias Stolpe

January 2017

DTU Vindenergi
Institut for Vindenergi

Author(s): Tibaldi C, Hansen H.M., Stolpe M.
Title: Analytical gradients of wint turbine towers fatigue loads.
Institute: Department of Wind Energy

Summary:
Optimization design procedure can have better convergence when provided with analytical gradients. Improvements are expected especially when the cost function or constraints depend on parameters that have a stochastic nature, such as wind turbulence.
This report presents a method to compute analytical gradients of fatigue loads on wind turbine towers. The approach is based on a spectral method that allows estimating the fatigue based on the power spectrum of the signal of interest. The spectrum is obtained from the transfer function of a linear model of the tower excited at the top by a force and a moment.
The report contains both the theory manual and the user manual.

Contents

1 Introduction

This report contains the user and theory manuals of the package that computes analytical gradients of tower bending moments fatigue damage rates.

The main goal of this method is to provide analytical gradients to tools that perform numerical optimization design of towers and supporting structures of wind turbines. Analytical gradients are expected to ease the convergence of optimization design processes compared to approaches where finite differences are used. Improvements are expected especially when the cost function or constraints depend on parameters computed from stochastic signals, such as the fatigue.

The fatigue is normally computed based on the rainflow counting of time domain signals, however, analytical derivatives of this approach cannot be computed because it relies on counting of cycles that is not differentiable. To overcome this issue, an approach that estimates the fatigue based on the power spectrum of a signal [1, 2] is here used. This method computes the fatigue damage rate based on an analytical function that depends on some of the power spectrum moments. All the steps in this procedure to estimate the fatigue are differentiable, therefore the gradients can be determined analytically.

The beam model that is used to represent the tower is implemented in HAWCStab2 [3, 4, 5, 6]. HAWCStab2 is an aeroelastic tool mainly used for wind turbine nonlinear steady-states computations and linear stability analysis. Furthermore, it computes and outputs a linear model of the wind turbine that can be used for further analysis.

The wind turbine linear models, obtained with HAWCStab2, have been already used in conjunction with the spectral method to compute the fatigue damage rate. A detail description of this method can be found in [7] and its applications within optimization design of wind turbines are described in [8, 9]. All the previous applications use finite differences to compute the gradients of the fatigue loads.

In this report the DTU 10 MW Reference Wind Turbine is used as a reference model [10, 11, 12].

1.1 Approach

This section describes the workflow used to estimate the fatigue. Figure 1.1 shows a diagram of the workflow. Each step is analytically derived, therefore analytical gradients can be obtained. The derivation of the analytical derivatives is shown in the next section.

Two sets of inputs are required to the method: the definition of the tower by the specification of outer radius $\mathbf{r}$ and wall thickness $\mathbf{t}$ at specific sections $\mathbf{z}$ and the time signal of external forces at the tower top $\mathbf{u}(t)$. The tower definition is used to compute the tower
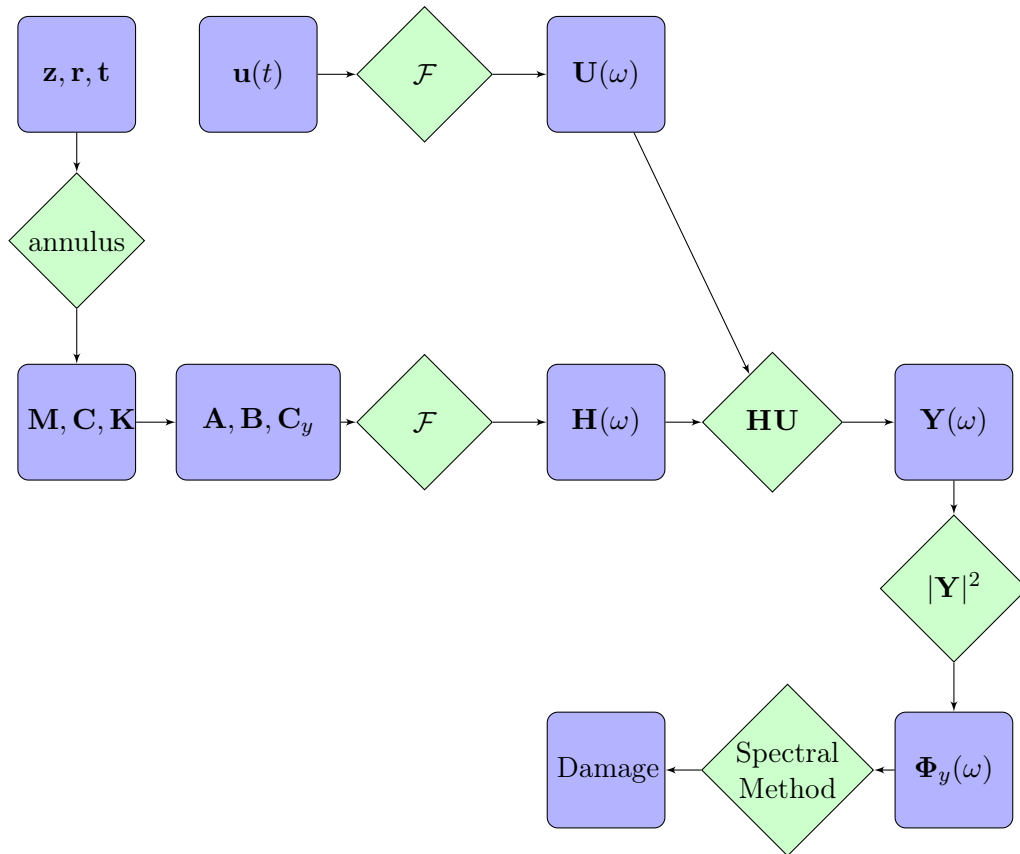
Figure 1.1: Block diagram of the workflow to compute the damage of the output starting from the definition of the tower based on radius and thickness and the time series of the external excitations.

structural properties and therefore the mass, damping and stiffness matrices. From these matrices, the first order state-space representation of the system is obtained, i.e. the matrices $\mathbf{A}, \mathbf{B}, \mathbf{C}_y$. The inputs to the system are a longitudinal force and a longitudinal bending moment acting at the tower top, representing the actions transmitted from the nacelle to the supporting structure. The outputs of the system are longitudinal bending moments at each section of the tower. The state-space representation allows to pass easily in frequency domain by computing the transfer function of the system $\mathbf{H}(\omega)$. The input time series $\mathbf{u}(t)$ are processed to obtain their frequency domain representation. The system transfer function and the input signal in frequency domain can be combined to obtain the representation of the outputs in frequency domain and, hence, their power spectra $\mathbf{\Phi}_y(\omega)$. The power spectra of the outputs is the only input to the spectral moment that allows estimating the damage rate.

1.2 Model simplifications

The current version of this method is based on the following assumptions and simplifications:

1. fatigue loads are computed based on a beam model, representing the tower, with a concentrated force and bending moment at the top. The beam model is divided into different bodies with nodes at the interfaces. The tower is fully clamped at its base. The rotor inertias are included into the model of the tower. The force and moment applied at the tower top need to be computed beforehand with an aeroelastic simulations and represent the internal forces that the nacelle is transferring to the supporting structure;

2. the structural properties of the tower are computed assuming annular sections. The sections are defined at the nodes by their position along the tower, a radius, and a thickness;

3. the tower beam model is linear;

4. fatigue loads are computed at any node of the beam model except the base one. The loads cannot be computed at locations between nodes;

5. the gradients of the structural damping are not implemented yet. Therefore, the gradients of the fatigue do not take into account changes in structural damping due to changes in the tower sections design.

1.3 Aerodynamic damping

Figure 1.2 shows the total damping of the first tower modes as function of wind speed. It is seen that the longitudinal mode has damping ratios between $6 - 11$ % and the lateral mode is less than 1 % damped. The two modes are equally damped structurally (0.6 % damping ratio), so the longitudinal mode must be significantly more damped by the aerodynamic forces than the lateral mode.

The model implemented in this version is purely structural and all the aerodynamic forces are introduced through the forces applied at the tower top. Because of the separation of the aerodynamics, the contribution to the damping to the tower modes is purely structural. Therefore the resulting damping of the longitudinal modes are lower than those obtained when the entire turbine and aerodynamic are considered. To compensate this gap a simple model has been implemented to compute the aerodynamic damping of the first longitudinal tower mode. This damping is then added to the structural damping matrix. The damping of the second mode and higher are increased by increasing the corresponding structural damping. The total damping of the tower modes can easily be defined the spectral damping model implemented in HAWCStab2.
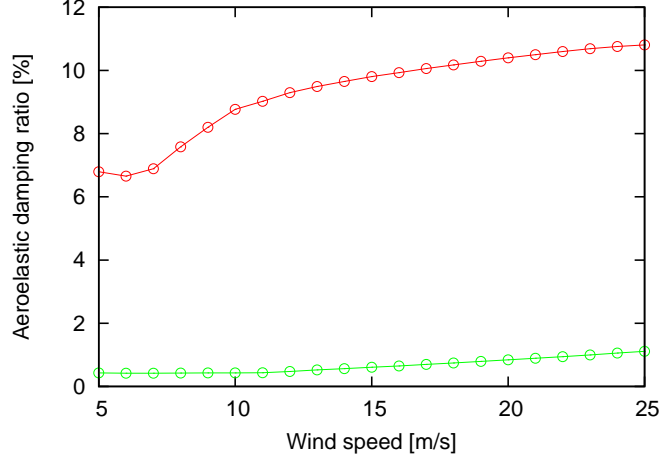
Figure 1.2: Total aeroelastic damping ratios of the first longitudinal and lateral tower
modes of the DTU 10MW reference wind turbine computed with HAWCStab2
for all operational wind speeds.

The aerodynamic force contributing to the damping of the first tower longitudinal mode
is modeled by linearizing the rotor thrust force for variation of the tower top velocity:

$$F_d = \frac{\partial T}{\partial V} \dot{x} \tag{1.1}$$

where F_d is the force contributing to the aerodynamic damping, T is the rotor thrust, V
is the mean wind velocity, and $\dot{x}$ is the longitudinal velocity of the tower top degree of
freedom. The derivative of the thrust can be expressed as:

$$\frac{\partial T}{\partial V} = \rho A V C_T \tag{1.2}$$

where ρ is the air density, A is the rotor radius, and C_T is the thrust coefficient. To add
the viscous damping force in (1.1) in the simplified model, this derivative is simply added
to the total damping matrix of the model as the damping coefficient.

The only unknowns to obtain the damping coefficient are the wind speed and the thrust
coefficient. At wind speeds below the full power region, the thrust coefficient is close to the
theoretical optimal value of approximately 0.89. When the power is regulated to its rated
value, the controller ensures that the blades are pitched out and the thrust coefficient
is reduced. The action of the controller is so slow (in fact to avoid excitation of the
tower mode) that the thrust coefficient can be assumed constant. Because the damping
coefficient (1.2) is the product of the thrust coefficient and the wind speed, it is a good
approximation to assume that this damping coefficient is constant; which can also be seen
in almost constant aeroelastic damping of the first longitudinal tower mode in Figure 1.2.

For the analysis of the DTU 10MW reference wind turbine in the following, the thrust
coefficient is set to 0.8 and the wind speed used for the computation of the damping
coefficient is 8 m/s. Using that the radius of the DTU 10 MW rotor is 89 m, and adding the
resulting damping coefficient into the damping matrix of the simplified tower model, a total

8   *DTU Wind Energy E-0138*

damping ratio of the first longitudinal tower is computed to be 7.1 %. This value is in the low end of the aeroelastic modal damping computed with HAWCStab2 (cf. Figure 1.2).

2 Analytical derivatives

This section contains the detail description of the method and the validation of the different individual steps of the workflow to compute the analytical gradients of the fatigue damage.

2.1 Tower beam structural properties

The tower is modeled as a beam with an annular cross section. The beam model implemented in HAWCStab2 requires the following inputs that are function of the shape:

- mass (m)
- radius of gyration (r_x, r_y)
- moment of inertia (I_x, I_y)
- torsional stiffens (K)
- area (A)

Their values for the section under consideration can be computed analytically and are:

$$m = \rho\pi(R^2 - r^2) \qquad\qquad r_x = r_y = \frac{1}{2}\sqrt{R^2 + r^2} \qquad (2.1)$$

$$I_x = I_y = \frac{\pi}{4}(R^4 + r^4) \qquad\qquad K = \frac{\pi}{2}(R^4 + r^4) \qquad (2.2)$$

$$A = \pi(R^2 + r^2) \qquad (2.3)$$

$$\qquad (2.4)$$

where ρ is the material density, R is the outer radius, and r is the inner radius. The inner radius r can also be expressed as $R - t$ where t is the wall thickness.

The variables R and t are selected as independent variables. The derivatives of the sectional properties with respect to the outer radius R are:

$$\frac{\partial m}{\partial R} = 2\rho\pi(R - r) \qquad\qquad \frac{\partial r_x}{\partial R} = \frac{\partial r_y}{\partial R} = \frac{1}{2}\frac{R + r}{\sqrt{R^2 + r^2}} \qquad (2.5)$$

$$\frac{\partial I_x}{\partial R} = \frac{dI_y}{dR} = \pi(R^3 - r^3) \qquad\qquad \frac{\partial K}{\partial R} = 2\pi(R^3 - r^3) \qquad (2.6)$$

$$\frac{\partial A}{\partial R} = 2\pi(R - r) \qquad (2.7)$$

and with respect to t are:

$$\frac{\partial m}{\partial t} = 2\rho\pi r \qquad\qquad \frac{\partial r_x}{\partial t} = \frac{\partial r_y}{\partial R} = -\frac{1}{2}\frac{r}{\sqrt{R^2 + r^2}} \qquad (2.8)$$

$$\frac{\partial I_x}{\partial t} = \frac{\partial I_y}{\partial R} = \pi r^3 \qquad\qquad \frac{\partial K}{\partial t} = 2\pi r^3 \qquad (2.9)$$

$$\frac{\partial A}{\partial t} = 2\pi r \qquad (2.10)$$

2.2 System mass and stiffness matrices

The gradients of the structural mass and stiffness matrices are implemented in HAWC-Stab2. For detail about the implementation please refer to the HAWCStab2 developer report. The gradients are actually implemented as a variation with respect to a general parameter p. All the structural inputs to the model are function of p. The way p affects all the input parameters is defined in an input file that is specified in the main htc file. Since the gradients are implemented with respect to a variation of one parameter, HAWCStab2 returns only the derivatives of the structural mass and stiffness matrices with respect to p.

The derivatives with respect to the structural damping matrix have not been implemented yet.

2.3 First order system

To compute the power spectrum of the system response, the system equation should first be written in the first order form:

$$\dot{\mathbf{x}} = \mathbf{A}\mathbf{x} + \mathbf{B}u \qquad (2.11a)$$

$$\mathbf{y} = \mathbf{C}_y\mathbf{x} \qquad (2.11b)$$

$$(2.11c)$$

where $\mathbf{A}$ is the system matrix, $\mathbf{B}$ the input matrix, and $\mathbf{C}_y$ the output matrix. The system matrix can be obtained as:

$$\mathbf{A} = \begin{bmatrix} 0 & \mathbf{I} \\ -\mathbf{M}^{-1}\mathbf{K} & -\mathbf{M}^{-1}\mathbf{C} \end{bmatrix}, \qquad (2.12)$$

where $\mathbf{M}$ is the mass matrix, $\mathbf{C}$ is the damping matrix, and $\mathbf{K}$ is the stiffness matrix. Given the derivatives of the mass and stiffness matrices, the derivatives with respect to the general parameter p of the first order formulation of the system can be computed as:

$$\frac{d\mathbf{A}}{dp} = \begin{bmatrix} 0 & 0 \\ \mathbf{M}^{-1}\frac{d\mathbf{M}}{dp}\mathbf{M}^{-1}\mathbf{K} - \mathbf{M}^{-1}\frac{d\mathbf{K}}{dp} & \mathbf{M}^{-1}\frac{d\mathbf{M}}{dp}\mathbf{M}^{-1}\mathbf{C} \end{bmatrix}, \qquad (2.13)$$

When the outputs are forces and moments at the nodes of the structure, the output matrix depends only on the stiffness matrix. In the current version of the tool, only the longitudinal bending moment is implemented as output.

$$\frac{d\mathbf{C}_y}{dp} = \frac{d\mathbf{K}}{dp} \tag{2.14}$$

The input matrix is a function of the mass matrix and a matrix that links the motion of each node $\mathbf{T}$. This second matrix is a result of the kinematic used in HAWCStab2 and does not depend on the input parameters. The derivative of the input matrix is:

$$\frac{d\mathbf{B}}{dp} = -\mathbf{M}^{-1}\frac{d\mathbf{M}}{dp}\mathbf{M}^{-1}\mathbf{T}\mathbf{b} \tag{2.15}$$

where $\mathbf{b}$ is a matrix with as many columns as the forces and moments set as inputs to the system. The matrix $\mathbf{b}$ is a sparse matrix with non zeros entries at the corresponding positions of the nodes where the force and moment are applied.

2.4 Power spectrum

The power spectrum of a signal can be computed from the transfer function of the system.

$$\mathbf{H}(\omega) = \mathbf{C}_y(j\omega\mathbf{I} - \mathbf{A})^{-1}\mathbf{B} \tag{2.16}$$

where j is $\sqrt{-1}$, ω the circular frequency, and $\mathbf{I}$ an identity matrix.

The derivative of the transfer function with respect to p is:

$$\frac{d\mathbf{H}(\omega)}{dp} = \frac{d\mathbf{C}_y}{dp}(j\omega\mathbf{I}-\mathbf{A})^{-1}\mathbf{B}+\mathbf{C}_y(j\omega\mathbf{I}-\mathbf{A})^{-1}\frac{d\mathbf{A}}{dp}(j\omega\mathbf{I}-\mathbf{A})^{-1}+\mathbf{C}_y(j\omega\mathbf{I}-\mathbf{A})^{-1}\frac{d\mathbf{B}}{dp} \tag{2.17}$$

Given the transfer function of the system the power spectrum of the outputs can be computed as:

$$\boldsymbol{\Phi}_y(\omega) = \mathbf{H}(\omega)^*\boldsymbol{\Phi}_u(\omega)\mathbf{H}(\omega) \tag{2.18}$$

where $\boldsymbol{\Phi}_u(\omega)$ are the power spectra of the input signals. The inputs here are assumed not be dependent on the design of the tower. The derivative of the power spectra are:

$$\frac{d\boldsymbol{\Phi}_y(\omega)}{dp} = \frac{d\mathbf{H}(\omega)^*}{dp}\boldsymbol{\Phi}_u(\omega)\mathbf{H}(\omega) + \mathbf{H}(\omega)^*\boldsymbol{\Phi}_u(\omega)\frac{d\mathbf{H}(\omega)}{dp} \tag{2.19}$$

2.5 Fatigue damage rate

The method that is used to evaluate the fatigue damage based on the spectrum of a signal is described in detail in [2, 1].

The method uses four moments of the PSD to evaluate the fatigue damage rate.

$$\lambda_0 = \int \Phi(f)df, \quad \lambda_1 = \int f\Phi(f)df, \quad \lambda_2 = \int f^2\Phi(f)df, \text{ and } \quad \lambda_4 = \int f^4\Phi(f)df \quad (2.20)$$

where f is the frequency. The derivatives with respect to the parameter p are:

$$\frac{d\lambda_0}{dp} = \int \frac{d\Phi(f)}{dp}df, \qquad\qquad \frac{d\lambda_1}{dp} = \int f\frac{d\Phi(f)}{dp}df, \qquad (2.21)$$

$$\frac{d\lambda_2}{dp} = \int f^2\frac{d\Phi(f)}{dp}df, \text{ and} \qquad \frac{d\lambda_4}{dp} = \int f^4\frac{d\Phi(f)}{dp}df \qquad (2.22)$$

$$(2.23)$$

Information from the spectral moments can be gathered in two parameters, the first and second bandwidth parameters:

$$\alpha_1 = \frac{\lambda_1}{\sqrt{\lambda_0\lambda_2}} \quad \text{and} \quad \alpha_2 = \frac{\lambda_2}{\sqrt{\lambda_0\lambda_4}} \qquad (2.24)$$

$$\frac{d\alpha_1}{dp} = \frac{1}{\lambda_0\lambda_2}\left[\frac{d\lambda_1}{dp}\sqrt{\lambda_0\lambda_2} - \frac{1}{2}\lambda_1(\lambda_0\lambda_2)^{-0.5}\left(\frac{d\lambda_0}{dp}\lambda_2 + \lambda_0\frac{d\lambda_2}{dp}\right)\right] \qquad (2.25)$$

$$\frac{d\alpha_2}{dp} = \frac{1}{\lambda_0\lambda_4}\left[\frac{d\lambda_2}{dp}\sqrt{\lambda_0\lambda_4} - \frac{1}{2}\lambda_2(\lambda_0\lambda_4)^{-0.5}\left(\frac{d\lambda_0}{dp}\lambda_4 + \lambda_0\frac{d\lambda_4}{dp}\right)\right] \qquad (2.26)$$

The rainflow fatigue damage rate (D) is computed as a combination of the damage rate of a narrow-banded process (D_{NB}) and of a range counting damage (D_{RC}), as

$$D = b_{wgt}D_{NB} + (1 - b_{wgt})D_{RC} \qquad (2.27)$$

where b_{wgt} is the weight

$$b_{wgt} = \frac{\alpha_1 - \alpha_2}{(\alpha_2 - 1)^2}\left[1.112(1 + \alpha_1\alpha_2 - \alpha_1 - \alpha_2)e^{2.11\alpha_2} + \alpha_1 - \alpha_2\right] \qquad (2.28)$$

The respective derivatives are:

$$\frac{dD}{dp} = \frac{db_{wgt}}{dp}D_{NB} + b_{wgt}\frac{dD_{NB}}{dp} - \frac{db_{wgt}}{dp}D_{RC} + (1 - b_{wgt})\frac{dD_{RC}}{dp} \qquad (2.29)$$

and

$$\frac{db_{wgt}}{dp} = \frac{(\frac{d\alpha_1}{dp} - \frac{d\alpha_2}{dp})(\alpha_2 - 1) - 2(\alpha_1 - \alpha_2)\frac{d\alpha_2}{dp}}{(\alpha_2 - 1)}\left[1.112(1 + \alpha_1\alpha_2 - \alpha_1 - \alpha_2)e^{2.11\alpha_2} + \alpha_1 - \alpha_2\right]+ \qquad (2.30)$$

$$+ \frac{\alpha_1 - \alpha_2}{(\alpha_2 - 1)^2}\left[2.346(1 + \alpha_1\alpha_2 - \alpha_1 - \alpha_2)\frac{d\alpha_2}{dp}e^{2.11\alpha_2} + \qquad (2.31)\right.$$

$$+ 1.112(\frac{d\alpha_1}{dp}\alpha_2 + \alpha_1\frac{d\alpha_2}{dp} - \frac{d\alpha_1}{dp} - \frac{d\alpha_2}{dp})e^{2.11\alpha_2} \qquad (2.32)$$

The range counting damage is approximated as a function of the damage of the narrow-banded process, the second bandwidth parameter α_2, and the m exponent.

$$D_{RC} \approx D_{NB}\alpha_2^{m-1} \tag{2.33}$$

the m exponent is here considered a constant, therefore, it does not depend on the input parameters

$$\frac{dD_{RC}}{dp} \approx \frac{dD_{NB}}{dp}\alpha_2^{m-1} + (m-1)D_{NB}\alpha_2^{m-2}\frac{d\alpha_2}{dp} \tag{2.34}$$

Finally the damage of a narrow-banded process is computed as

$$D_{NB} = \frac{\nu_0}{S_0^m}\left(\sqrt{2\lambda_0}\right)^m \Gamma(1 + 0.5m) \tag{2.35}$$

where Γ is the Gamma function, S_0 is the critical stress level, and ν_0 is the rate of mean upcrossings. The last parameter can be computed as

$$\nu_0 = \frac{1}{2\pi}\frac{\sqrt{\lambda_2}}{\lambda_0} \tag{2.36}$$

The derivative of D_{NB} can be computed as:

$$\frac{dD_{NB}}{dp} = \left[(2\lambda_0)^{\frac{m}{2}}\frac{d\nu_0}{dp} + m\nu_0(2\lambda_0)^{\frac{m}{2}-1}\frac{d\lambda_0}{dp}\right]\frac{\Gamma(1 + 0.5m)}{S_0^m} \tag{2.37}$$

and finally the one of ν_0

$$\frac{d\nu_0}{dp} = \frac{1}{2\pi\lambda_0^2}\left(\frac{\lambda_0}{2\sqrt{\lambda_2}}\frac{d\lambda_2}{dp} - \sqrt{\lambda_2}\frac{d\lambda_0}{dp}\right) \tag{2.38}$$

2.6 Verification

This section shows the verification of the analytical derivatives of the main steps of the workflow. The verification is performed against finite differences using the same model.

Figure 2.1 shows the differences between the analytical derivatives and the finite differences derivatives of the entries of the mass and stiffness matrices. For clarity a tower model composed by 3 bodies is used such that the matrices are not too large. With 3 bodies the matrices have 324 entries. The plots show the gradients with respect to the tower wall thickness and radius. The perturbations at the 4 different nodes are shown overlapped on the same plots. Finite differences and analytical gradients show very similar results.

a) Mass matrix w.r.t. thickness.

b) Mass matrix w.r.t. radius.

c) Stiffness matrix w.r.t. thickness.

d) Stiffness matrix w.r.t. radius.
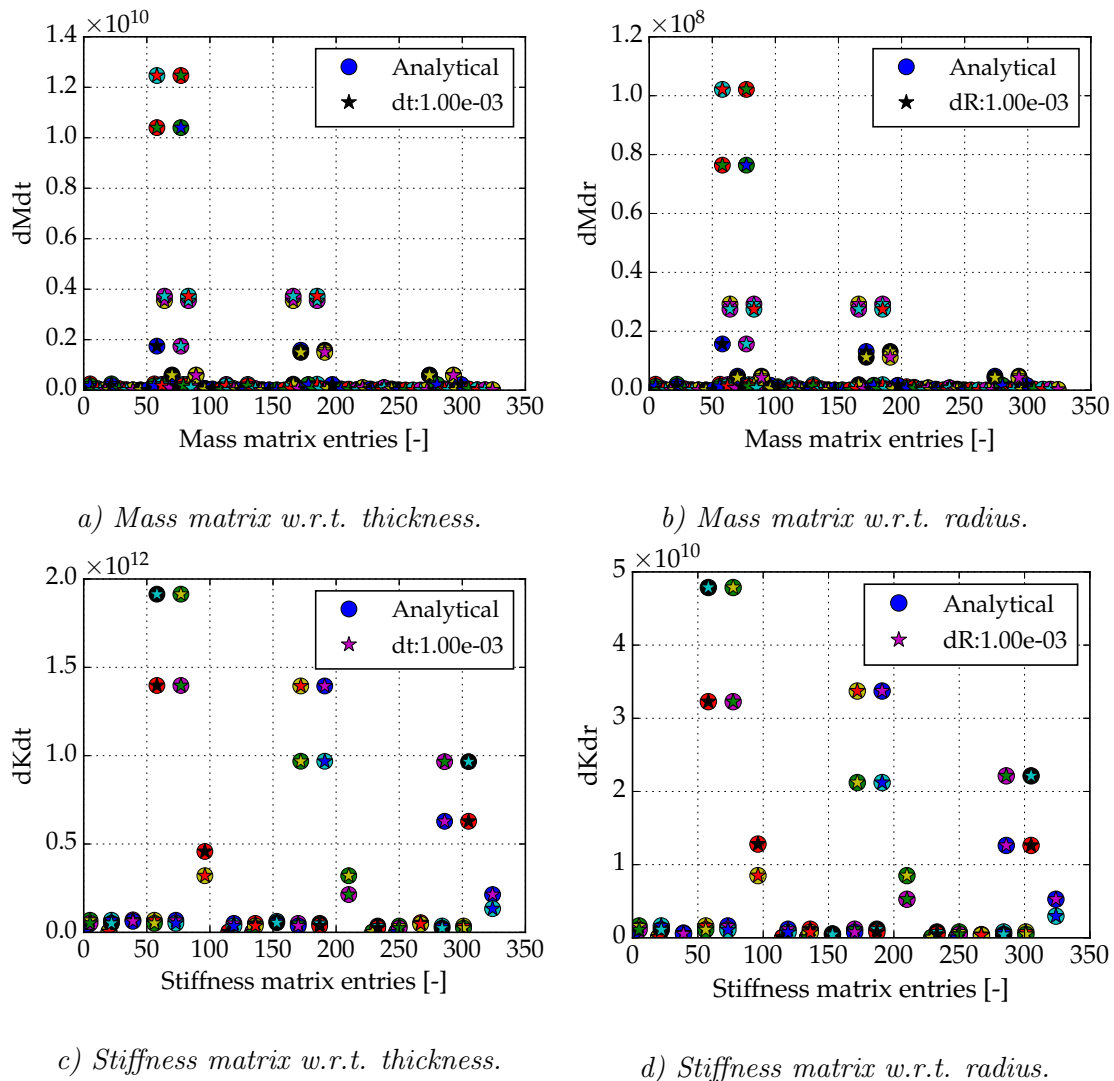
Figure 2.1: Derivative of mass and stiffness matrices entries with respect to the tower wall thickness and radius. Tower model composed by 3 bodies. Radius and thickness variations at the different sections are shown on the same plot.

Figure 2.2 shows the difference between the analytical derivatives and the finite differences derivatives of the module of the system transfer function from tower top longitudinal force to tower longitudinal bending moment at 7.7m from the bottom. The derivatives are computed perturbing wall thickness and radius at 0, 53.96, and 115.63m. The tower model is composed of 15 bodies. The derivatives are shown only up to 5Hz. The gradient has highest module around the first tower frequencies. Analytical and finite differences agree very well close to the first tower mode frequency. At higher frequencies values, when the value of the derivatives is smaller, the derivatives have larger differences. However, the general behavior is captured.

Figure 2.3 shows the same as Figure 2.2 but for a sensor at the tower top. Also in this case a good agreement is obtained, since at each frequency the difference between the two spectra in not large. However, when the parameters at the tower top section are changed, cases *e* and *f*, the spectra of the derivative does not have a dominant peak in proximity of the first longitudinal tower frequency anymore. Therefore, the moments of the two spectra are significantly different. This error is going to have a strong effect on the derivatives of the fatigue since the spectral method relies only on the spectral moments. This issue should be reduced implementing the analytical derivatives also of the damping matrix.

Figure 2.5 shows the comparison between analytical and finite differences derivatives of the damage of three different sensors with respect to variations of tower wall thickness and radius at several position along the tower. The damage is computed at 7.71, 61.67, and 115.6m. The tower model is composed of 15 bodies. A sinusoidal signal with frequency of 0.1Hz is used as longitudinal excitation. Close to the base and at mid tower the estimation of the derivatives fits very well with the finite differences. Close to the tower top the difference becomes significant. This difference comes directly from the error seen in the transfer functions derivatives, due to the differences in the damping.
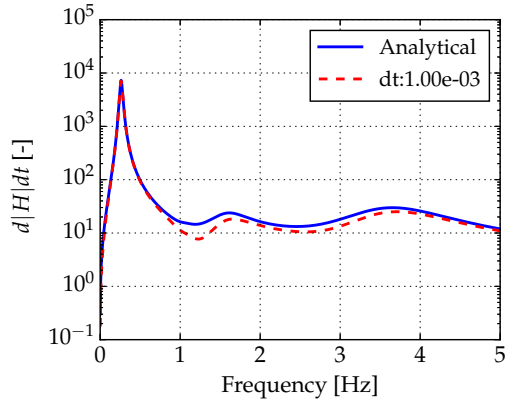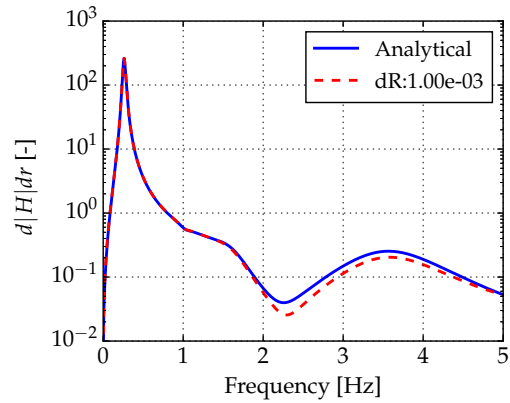
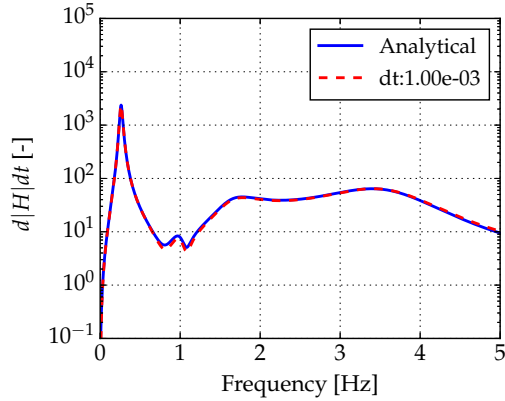a) *Derivative at 7.71m w.r.t. thickness at 0m.*
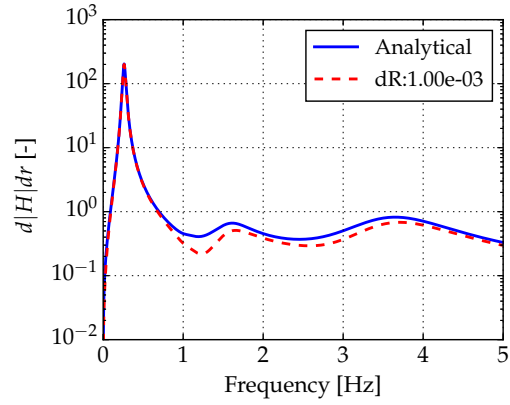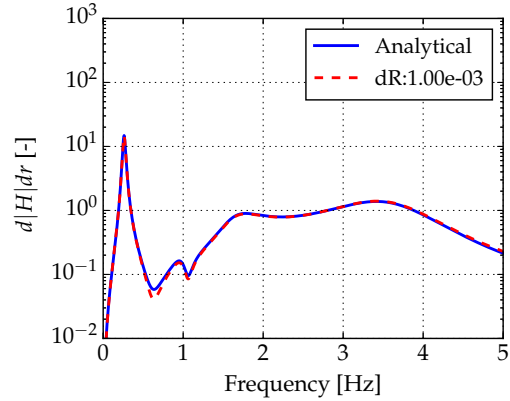
b) *Derivative at 7.71m w.r.t. radius at 0m.*
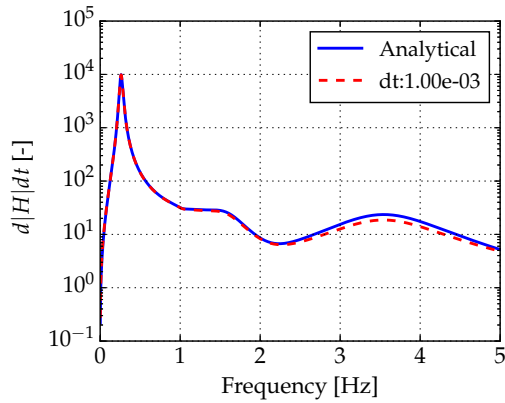
c) *Derivative at 7.71m w.r.t. thickness at 53.96m.*

d) *Derivative at 7.71m w.r.t. radius at 53.96m.*

e) *Derivative at 7.71m w.r.t. thickness at 115.63m.*
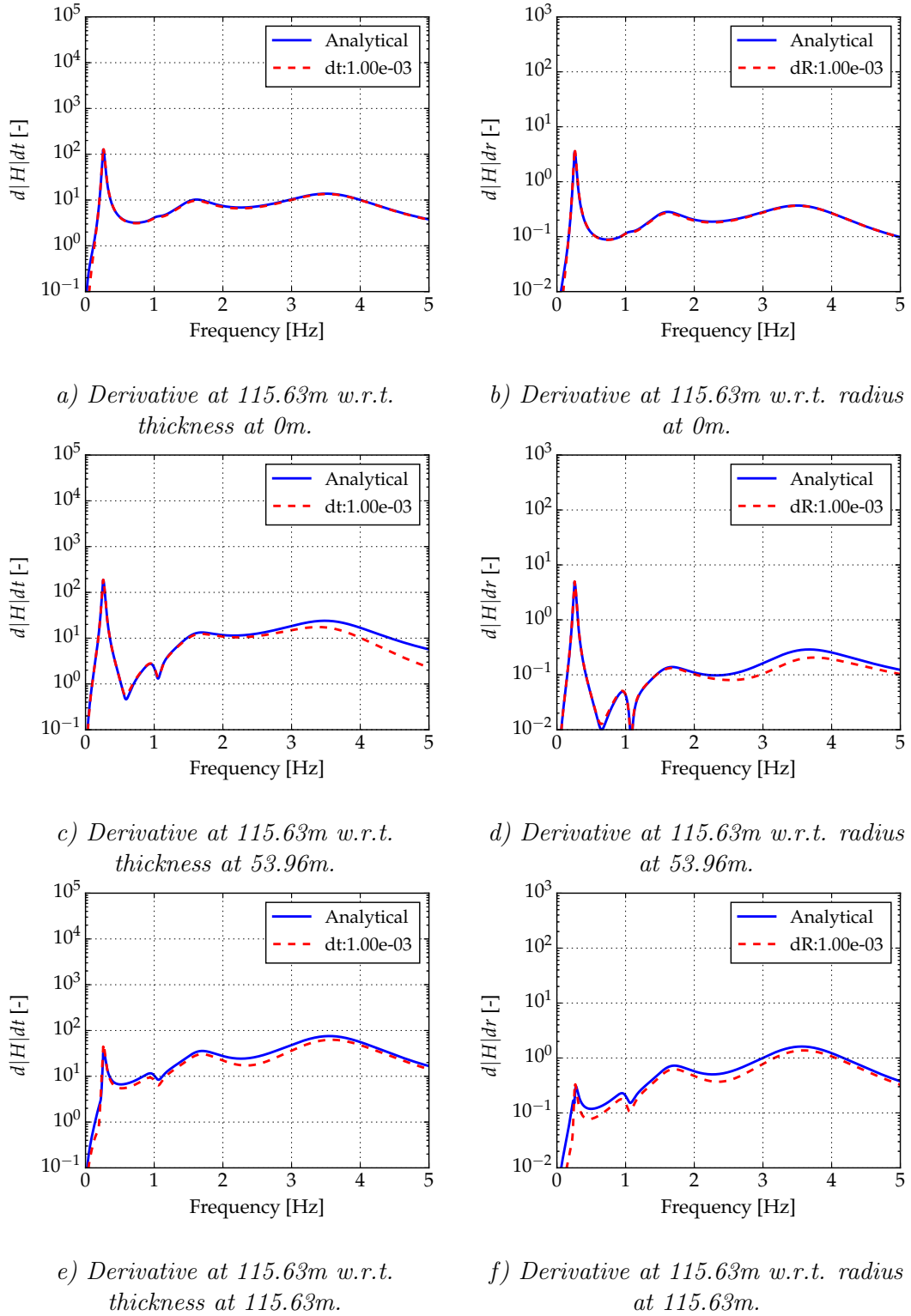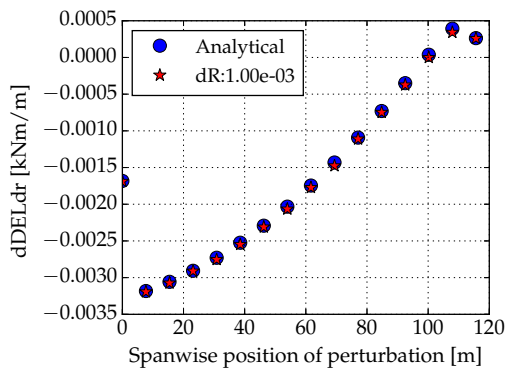
f) *Derivative at 7.71m w.r.t. radius at 115.63m.*

Figure 2.2: Derivative of the transfer function module with respect to variations of the tower wall thickness and radius at different tower heights. Transfer function from longitudinal force at the tower top to longitudinal bending moment at 7.7m from the bottom. Tower model composed by 15 bodies.
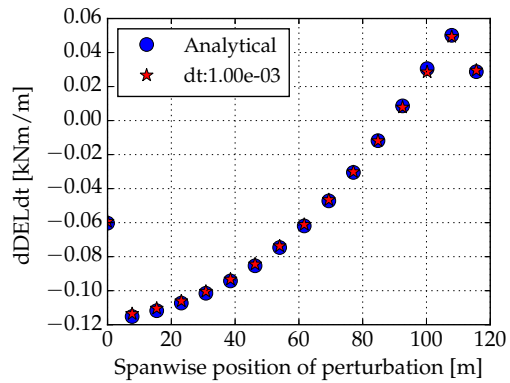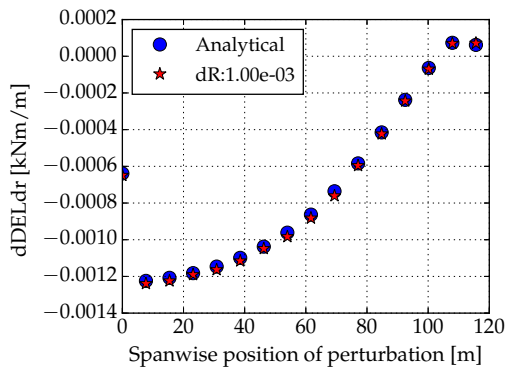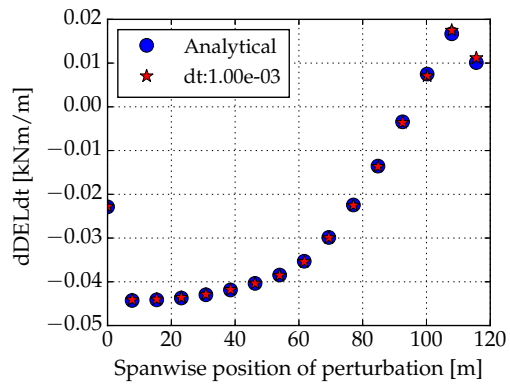
a) Derivative at 115.63m w.r.t.
thickness at 0m.

b) Derivative at 115.63m w.r.t. radius
at 0m.

c) Derivative at 115.63m w.r.t.
thickness at 53.96m.

d) Derivative at 115.63m w.r.t. radius
at 53.96m.

e) Derivative at 115.63m w.r.t.
thickness at 115.63m.

f) Derivative at 115.63m w.r.t. radius
at 115.63m.

Figure 2.3: Derivative of the transfer function module with respect to variations of the tower wall thickness and radius at different tower heights. Transfer function from longitudinal force at the tower top to longitudinal bending moment at 115.63 from the bottom. Tower model composed by 15 bodies.

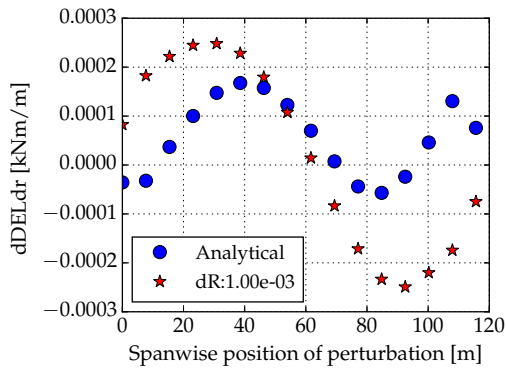a) Derivative at 7.71m w.r.t. thickness.
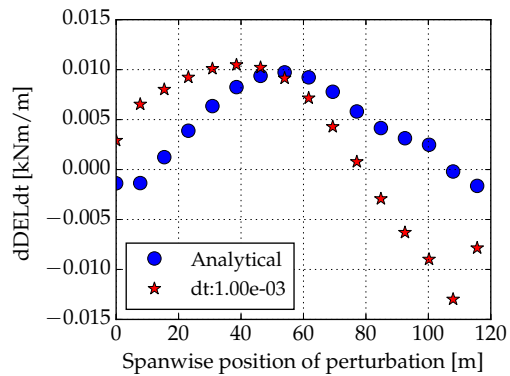

b) Derivative at 7.71m w.r.t. radius.

c) Derivative at 61.67m w.r.t. thickness.

d) Derivative at 61.67m w.r.t. radius.

e) Derivative at 115.6m w.r.t. thickness.

f) Derivative at 115.6m w.r.t. radius.

Figure 2.4: Derivative of the damage equivalent load with respect to variations of the tower wall thickness and radius at different tower heights. Derivative computed with perturbations at each tower node. Loads computed at 7.71, 46.25, and 84.8m. Tower excited by a sinusoidal longitudinal force of 0.1Hz at the tower top. Tower model composed by 15 bodies.

2.7 Validation

This section shows a comparison of the fatigue computed with the model here introduced and results obtained from nonlinear aeroelastic simulations performed with HAWC2 [13].

The loads in this section are computed for a single wind speed of 10m/s and one turbulence seed. The time series used as input to the linear model has been obtained from a simulation with stiff tower, to avoid having a content at the tower frequency in the input forces due to the longitudinal tower displacement.

Figure 2.5 a) shows a comparison of the fatigue damage rate computed with the spectral method and the rainflow counting damage equivalent load. Both fatigue indexes are obtained from the same time series obtained from a nonlinear aeroelastic simulation. The loads a re shown along the tower. Both loads are normalized with respect to their own value at the tower root. The plot shows that the spectral method is perfectly able to capture the variation of the fatigue loads along the tower. Figure 2.5 b) shows a comparison of fatigue damage rate computed with the spectral method with the linear model, introduced in this report, and nonlinear aeroelastic simulations. The figure shows that the linear model is capable of capturing the same load variation as the nonlinear model. The linear model overestimates the fatigue damage along the entire tower. This difference is attributed to the difference damping of the first longitudinal tower mode. A finer tuning of the damping would give closer results.

Figures 2.6 and 2.7 show the comparison of fatigue damage rate gradients at different positions along the tower obtained with finite differences of nonlinear simulations and the linear analytical method. Each plot show how the loads changes due to a perturbation
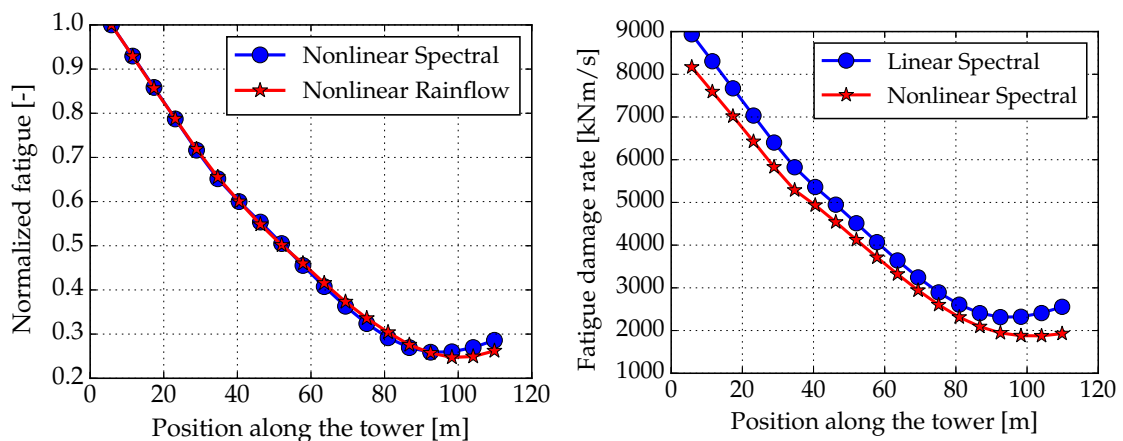

a) *Linear model with spectral method vs nonlinear model with Rainflow counting.*

b) *Linear model with spectral method vs. nonlinear model with spectral method.*

Figure 2.5: Comparison of the fatigue estimation obtained from the simplified model used in this method and nonlinear wind turbine aeroelastic simulations. The fatigue for the nonlinear model is estimated both with the spectral method from the power spectrum of the time series and with Rainflow counting.

at the different nodes. Both models use the spectral method to estimate the fatigue. The results in Figure 2.6 shows a very good agreement between the two models, both in quantitative and qualitative terms. Figure 2.7 shows the results for the loads at two sections close to the tower top. In these cases the differences between the linear and the nonlinear models are more significant, especially for perturbation very close to the tower top. The reason of these differences relies on the differences in damping between the two models and on the fact that in this version of the tool the analytical derivatives of the damping are not computed.
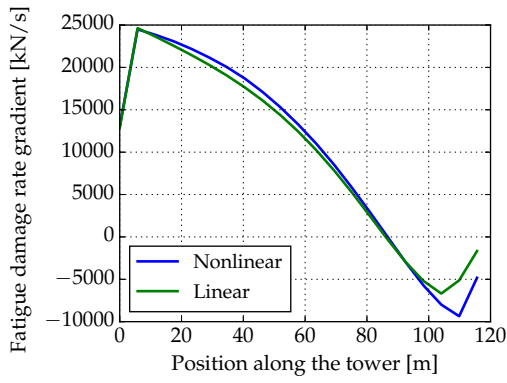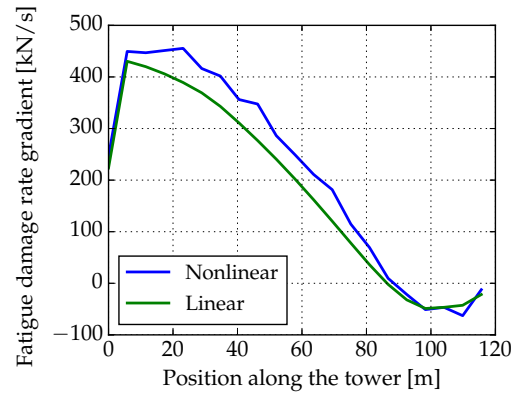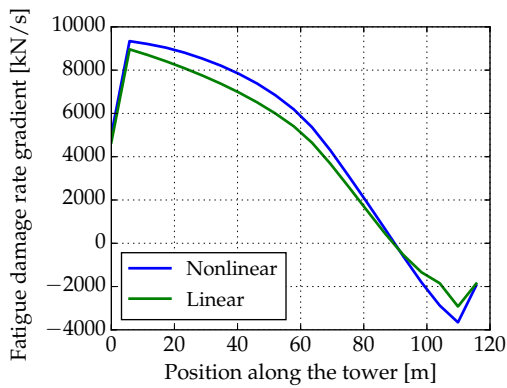
a) Derivative at 5.8m w.r.t. thickness.
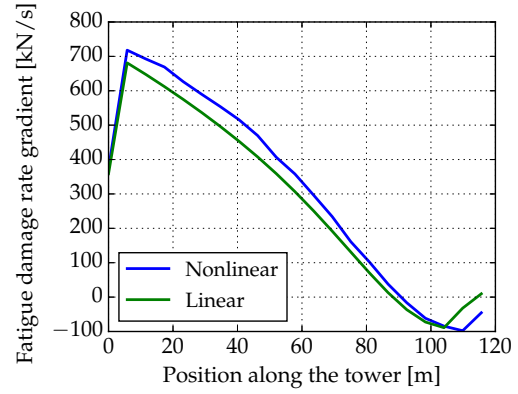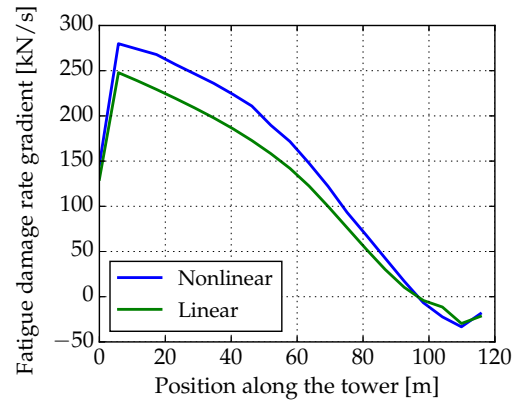
b) Derivative at 5.8m w.r.t. radius.
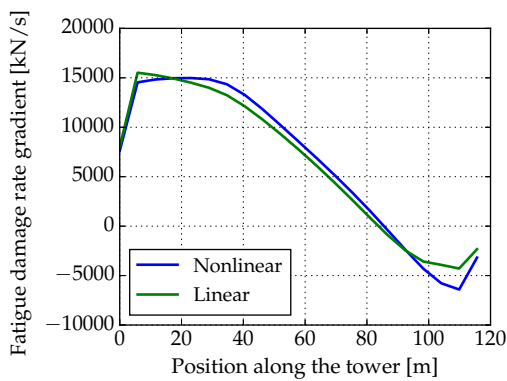
c) Derivative at 34.7m w.r.t. thickness.

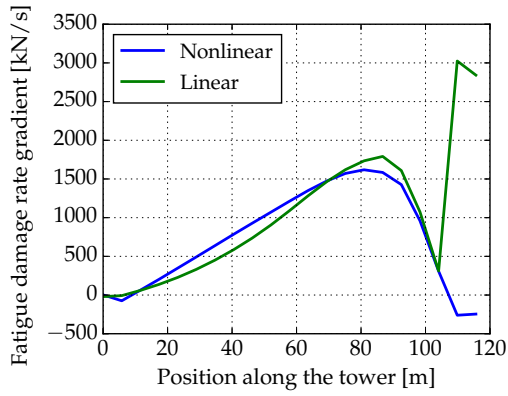*d) Derivative at 34.7m w.r.t. radius.*

e) Derivative at 63.6m w.r.t. thickness.

f) Derivative at 63.6m w.r.t. radius.

Figure 2.6: Derivative of the damage equivalent load with respect to variations of the tower wall thickness and radius at different tower heights. Comparison between finite differences of nonlinear simulations and the linear analytical method. Derivative computed with perturbations at each tower node. Loads computed at 5.8, 34.7, and 63.6m. Tower model composed by 15 bodies.

a) Derivative at 92.5m w.r.t. thickness.

b) Derivative at 92.5m w.r.t. radius.

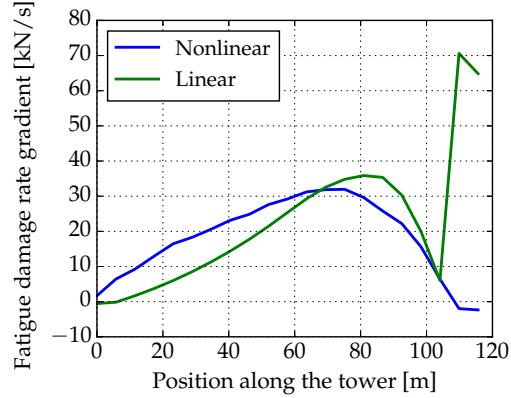c) Derivative at 109.85m w.r.t.
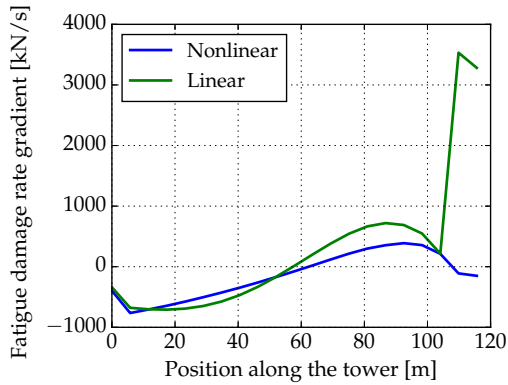thickness.

d) Derivative at 109.85m w.r.t. radius.

Figure 2.7: Derivative of the damage equivalent load with respect to variations of the tower wall thickness and radius at different tower heights. Comparison between finite differences of nonlinear simulations and the linear analytical method. Derivative computed with perturbations at each tower node. Loads computed at 92.5, and 109.8m. Tower model composed by 15 bodies.
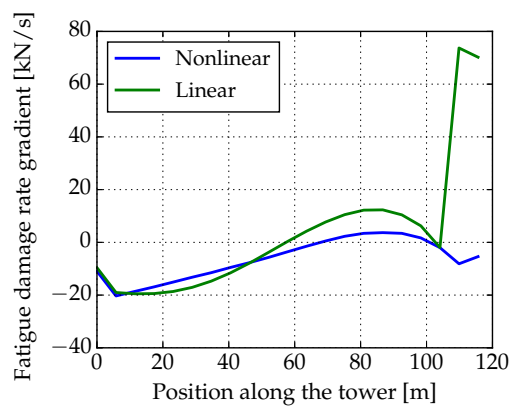
3 Manual

The package containing the method to compute the gradients of the fatigue is mainly programmed in Python. To facilitate the usage the tool is compiled into an executable that is interfaced with a Matlab function.

The code and the developer manual are in the repository

`https://gitlab.windenergy.dtu.dk/tlbl/TowerFatigueGradients`

The HAWCStab2 version required is contained in the repository

`https://gitlab.windenergy.dtu.dk/HAWCStab2/HAWCStab2/tree/tlbl`

3.1 Content of the folder

The distributed zip file contains the following:

bin This folder contains the HAWCStab2 executable and its license manager dll.

data This folder contains the data input files of the HAWCStab2 model of the wind turbine. The files `Gradient_TWR_simple.dat` and `DTU_10MW_RWT_Tower_st_input.dat` are modified by the tool accordingly. The files contained in this folder should be changed only if the reference turbine is changed.

tower_grad This folder contain the actual package to compute the gradients. Here, the files are all compiled and no source code is present.

hawc2s_input.htc This is the main HAWCStab2 input file. This file should be changed only if the reference turbine is changed.

FatigueGradients.m This file is the Matlab interface function. The function receives as inputs the positions along the tower of the nodes, the radius at the nodes and the wall thickness at the nodes. The function returns the fatigue damage rate and its derivatives with respect to the radius and thickness.

loads.dat This file contains the time history of the tower top force and moment that are used as excitation. This file is also an input to the the tool.

3.2 How to run it

Before running, it is best to check if HAWCStab2 is allowed to run on the current machine. To do so, open a command window in the folder bin and type `hawc2s+dummy` if an error message appear it means that a new license is required. Please contact hawcstab2@vindenergi.dtu.dk to get further information. If only the version number of HAWC-Stab2 appears it means that the license is accepted.

Once the license has been checked the tool can be executed by calling the Matlab function `FatigueGradients` directly from its folder. Note, therefore, that it is not possible yet to simply add the folder to the path and run the function from elsewhere because of some internal path definition.

4 Future development

The method here described can be further improved. The main differences between the method here presented and direct analysis of time domain nonlinear aeroelastic simulations occur for the derivatives of the fatigue close to the tower top. At this location, the assumption of neglecting the derivative of the structural damping matrix leads to too large errors. However, this deficit appears only very close to the top and does not affect the rest of the derivatives.

The following steps should be the focus of future developments:

- implement the derivative of the structural damping matrix to improve the estimation of the analytical derivatives;

- implement the calculation of the derivatives of the state space mode directly in HAWCStab2 to include the aerodynamics and avoid the tuning of the aerodynamic damping;

- link other external excitations to the mode, e.g. wave forces;

Bibliography

[1] D. Benasciutti and R. Tovo. Comparison of spectral methods for fatigue analysis of broad-band Gaussian random processes. *Probabilistic Engineering Mechanics*, 21(4): 287–299, October 2006. ISSN 0266-8920. doi: 10.1016/j.probengmech.2005.10.003. URL http://www.sciencedirect.com/science/article/pii/S0266892005000718.

[2] D. Benasciutti and R. Tovo. Spectral methods for lifetime prediction under wide-band stationary random processes. *International Journal of Fatigue*, 27(8):867–877, August 2005. ISSN 0142-1123. doi: 10.1016/j.ijfatigue.2004.10.007. URL http://www.sciencedirect.com/science/article/pii/S0142112305000617.

[3] http://hawcstab2.vindenergi.dtu.dk.

[4] M. H. Hansen. Aeroelastic stability analysis of wind turbines using an eigenvalue approach. *Wind Energy*, 7(2):133–143, 2004. ISSN 1099-1824. doi: 10.1002/we.116. URL http://onlinelibrary.wiley.com/doi/10.1002/we.116/abstract.

[5] M. H. Hansen. Aeroelastic Properties of Backward Swept Blades. pages 1–19, Orlando, Florida, 2011. American Institute of Aeronautics and Astronautics. doi: 10.2514/6. 2011-260.

[6] Ivan Sønderby and Morten H. Hansen. Open-loop frequency response analysis of a wind turbine using a high-order linear aeroelastic model. *Wind Energy*, 17(8):1147–1167, 2014. ISSN 1099-1824. doi: 10.1002/we.1624. URL http://dx.doi.org/10.1002/we.1624.

[7] C. Tibaldi, L. C. Henriksen, M. H. Hansen, and C. Bak. Wind turbine fatigue damage evaluation based on a linear model and a spectral method. *Wind Energy*, 19(7):1289–1306, July 2016. ISSN 10954244. doi: 10.1002/we.1898. URL http://doi.wiley.com/10.1002/we.1898.

[8] F. Zahle, C Tibaldi, DR Verelst, C Bak, R Bitsche, and JP Blasques. Aero-Elastic Optimization of a 10 MW Wind Turbine. American Institute of Aeronautics and Astronautics, 2015. ISBN 978-1-62410-344-5.

[9] T.K. Barlas, C. Tibaldi, F. Zahle, and H. Madsen. Aeroelastic optimization of a 10 MW wind turbine blade with active trailing edge flaps. 2016. ISBN 978-1-62410-395-7.

[10] Christian Bak, Robert Bitsche, Anders Yde, Taeseong Kim, Morten Hartvig Hansen, Frederik Zahle, Mac Gaunaa, José Pedro Albergaria Amaral Blasques, Mads Døssing, Jens-Jakob Wedel Heinen, and Tim Behrens. Light Rotor: The 10-MW reference wind turbine. *Proceedings of EWEA 2012 - European Wind Energy Conference & Exhibition*, 2012.

[11] C Bak, F. Zahle, R Bitsche, T. Kim, Anders Yde, LC Henriksen, Anand Natarajan, and M. H. Hansen. Description of the DTU 10 MW Reference Wind Turbine. Technical Report I-0092, DTU Wind Energy, Roskilde, Denmark, 2013.

[12] The DTU 10mw Reference Wind Turbine Project Site. URL dtu-10mw-rwt.vindenergi.dtu.dk.

[13] Torben J. Larsen and Anders Melchior Hansen. How 2 HAWC2, the user's manual. Technical Report Risø-R-1597(ver. 4-5)(EN), Risø National Laboratory, 2014. URL www.hawc2.dk.

DTU Wind Energy

DTU Wind Energy is a department of the Technical University of Denmark with a unique integration of research, education, innovation and public/private sector consulting in the field of wind energy. Our activities develop new opportunities and technology for the global and Danish exploitation of wind energy. Research focuses on key technical-scientific fields, which are central for the development, innovation and use of wind energy and provides the basis for advanced education at the education.

We have more than 230 staff members of which approximately 60 are PhD students. Research is conducted within 9 research programmes organized into three main topics: Wind energy systems, Wind turbine technology and Basics for wind energy.